

Noncooperative Precoding for Massive MIMO HetNets: SILNR Maximization Precoding

Deokhwan Han and Namyoon Lee

Department of Electrical Engineering, POSTECH, South Korea

Emails: {dhhan,nylee}@postech.ac.kr

Abstract—Massive multi-input multiple-out (MIMO) is a key ingredient in improving the spectral efficiencies for next-generation cellular systems. Thanks to the channel reciprocity, in time-division-duplexing mode, each base station (BS) can acquire local channel state information at the transmitter (CSIT) for a set of users possibly located in adjacent cells. When the small cell BSs equipped with not-so-many antennas are densely deployed with macrocells, a simple noncooperative MIMO precoding technique using local CSIT fails to achieve high spectral efficiency because of strong inter-cell-interference (ICI). In this paper, we present a novel noncooperative massive MIMO precoding technique called signal-to-interference-plus-leakage-plus-noise-ratio (SILNR) maximization precoding. The key idea of the proposed precoding is to jointly find a scheduled user set per cell, the beamforming vectors for the users, and the allocated power by simultaneously mitigating both inter-user-interference (IUI) and ICI leakage power using local CSIT. To accomplish this, we present a low-complexity algorithm that finds a local-optimal solution of the maximization problem for a lower bound of the sum spectral efficiency, i.e., a non-convex optimization problem. By system-level-simulations, we show that the proposed precoding method considerably outperforms the existing noncooperative precoding techniques in terms of the ergodic spectral efficiencies and rate distributions per user.

I. INTRODUCTION

Heterogeneous cellular networks (HetNets) are promising solutions for achieving ubiquitously high data rates [1]–[5]. HetNets are comprised of distinct network tiers, each with different transmission power and number of antennas. By deploying low power base stations (BSs) (called pico/femto cells) overlaid onto macrocells in the areas of a high user density, HetNets considerably increase area spectral efficiency by cell-splitting gains. When operating these small BSs using the same frequency/time resources with macro-cells, significant intra-tier and inter-tier interference problems can occur. This interference problem makes the area spectral efficiency gains sharply disappear. As a result, an effective interference mitigation technique is necessary to obtain the area spectral efficiency gains in HetNets [6]–[8].

Massive multi-input multiple-output (MIMO) is an effective solution to resolve this interference problem by exploiting a large degrees of freedom in the spatial domain [9]–[11]. With time-division-duplexing (TDD) operation, it has shown in the seminal paper [12] that simple precoding techniques with perfect channel state information at the transmitter (CSIT) are sufficient to completely eliminate both inter-user-interference (IUI) and inter-cell-interference (ICI) when using an infinite number of antennas. This result implies that non-cooperative

precoding with perfect CSIT of the associated users in a cell can be asymptotically optimal when the number of antennas is sufficiently larger than that of active downlink users per cell [13]. In HetNets, however, the number of antennas of BSs in small-cells cannot be large due to cost and hardware constraints [1]–[3]. Besides, the density of active users in the hotspots is relatively high. This fact fails to meet the commonly assumed condition to successfully eliminate both ICI and IUI using simple precoding techniques in massive MIMO HetNets [12], [13].

In this paper, we consider massive MIMO HetNets, in which the massive MIMO macro-cell tier is overlaid with small-cells, each equipped with not-so-many antennas. We assume that the user density at the small-cell areas is higher than that in the other regions in the cell, i.e., the channel hardening effects are not pronounced. We also assume that each small/macro-cell BS is available to have local CSIT for a set of users who use orthogonal uplink pilots. In this setting, we aim at finding a noncooperative precoding method that fully exploits local CSIT to achieve non-trivial gains over the existing linear precoding techniques. From this, we demonstrate that the synergetic gains are possible when massive MIMO meets HetNets.

A. Prior Works

There are extensive prior studies for multicell linear precoding methods using local CSIT. The simplest method is maximum ratio transmission (MRT) [14], which is also known as matched filtering (MF) precoding. To employ MRT, each BS only requires to have the local CSIT of its cell. In a multicell massive MIMO setting, where the number of BS antennas is much larger than that of users, the seminal work [12] has demonstrated that this simple precoding can asymptotically eliminate both IUI and ICI under perfect local CSIT assumption. Thanks to its simple precoding structure, the analytical expressions for achievable rates have been derived in closed-forms as a function of relevant system parameters in massive MIMO settings [15], [16]. For instance, using these expressions, the optimal ratio between the number of antennas and users has been found to maximize the energy efficiency (EE) of massive MIMO systems when applying MRT method. Although this scheme is simple to analyze the achievable spectral efficiencies, it does not fully exploit knowledge of CSIT towards other cell users. This fact can give rise to significant both IUI and ICI when the number of antennas per

BS is not-so-large. This method is limited to use for mitigating both IUI and ICI for massive MIMO HetNets.

Zero-forcing (ZF) [17] is another popular precoding method to eliminate IUI using local CSIT. Unlike MRT precoding, it can completely remove IUI regardless of the number of BS antennas by selecting the number of users that is not larger than that of BS. Particularly, when the number of users is sufficiently larger than the number of BS antennas, ZF precoding with semi-orthogonal user selection [18] has shown to asymptotically achieve the optimal capacity scaling law attained by [19] (DPC). In a massive MIMO setup, in which a BS has an infinite number of antennas, ZF precoding can be optimal for maximizing the sum spectral efficiency under the perfect CSIT assumption [12]. When the BS has not-so-large number of antennas compared to the number of users such as HetNets [1], [2], [20], ZF precoding is not effective to mitigate both IUI and ICI simultaneously because of the inefficient utilization of the spatial degrees of freedom.

Signal-to-leakage-plus-noise-ratio (SLNR) maximization precoding [21] is an effective method to suppress IUI using local CSIT in a single-cell MU-MIMO systems. In multicell MIMO networks, this SLNR maximization precoding has been extended to mitigate both IUI and ICI simultaneously based on local CSIT. This precoding solution has shown to be equivalent to the multi-cell minimum mean square error (M-MMSE) precoding [22]–[24], which is motivated by uplink-downlink duality. Recently, in cell-free massive MIMO systems [25], multicell SLNR precoding (or the M-MMSE precoding) has shown to be an attractive precoding method because of its scalability and ICI mitigation capability. The major limitation is that SLNR maximization precoding (or the M-MMSE precoding) does not necessarily maximize the sum spectral efficiency per cell.

The sum spectral efficiency maximization precoding techniques have extensively proposed in single-cell multi-user MIMO systems [22], [26]–[28]. Unfortunately, finding the optimal precoding solution to maximize the sum spectral efficiency is well-known as an NP-hard problem. Instead, some precoding algorithms that identify a local-optimal solution has been proposed. The most popular technique for maximizing the spectral efficiency is the weighted MMSE precoding [26]. Using the equivalent between the sum spectral efficiency maximization problem and the weighted MMSE problem with proper weights, the weighted MMSE precoding algorithm has shown to find a local-optimal solution via an alternative minimization algorithm. This precoding, however, cannot apply to a massive MIMO system because it requires very high computational complexity, i.e., it uses the second-order cone programming (SOCP) per iteration. Recently, inspired by principal component analysis (PCA), a novel low-complexity algorithm called generalized power iteration precoding (GPIP) has been presented, which guarantees a local-optimal solution for the sum spectral efficiency maximization problem [27], [28]. This precoding method has also been extended to a multicell scenario with pilot contamination effects [28]. This multicell precoding method, however, requires the BS cooperation using global CSIT.

B. Contributions

The main contributions of this paper are summarized as follows:

- We introduce a new performance metric to effectively mitigate both IUI and ICI in a distributed manner using local CSIT for massive MIMO HetNets. The new performance metric is signal-to-interference-pulse-leakage-pulse-noise-ratio (SILNR). The intuition behind this new metric stems from the controllability of IUI and ICI from a BS perspective under local CSIT knowledge. Using precoding with local CSIT knowledge, each BS can control 1) the desired signal power for intended users, 2) IUI power received at the users in the cell, and 3) the ICI leakage power towards the other cell users. Each BS, however, cannot control the ICI received at the users in the cell due to the absent of BS cooperation. Each user treats the ICI received from the other BSs' transmission as additional noise. As a result, SILNR per user is a measure of the ratio between the desired signal power and the sum of IUI, ICI leakage, and the effective noise power. This metric simplifies to the SINR when ignoring the ICI leakage power. Besides, it also becomes SLNR, when we replace IUI power into intra-cell interference leakage power.
- We present a novel massive MIMO precoding technique using local CSIT called SILNR maximization precoding. Unlike the M-MMSE precoding, our precoding strategy aims at finding a joint solution for the scheduled-user set, beamforming vectors, and the allocated power to maximize a lower bound of the sum spectral efficiencies using local CSIT. Unfortunately, the maximization of the lower bound is a well-known non-convex (and even NP-hard) problem. To design the precoding method, we first derive the first- and the second-order necessary conditions of a local-optimality for this non-convex optimization problem. Using the derived conditions, we present a low-complexity iterative algorithm that guarantees to converge a locally-optimal solution for the scheduled-user set, beamforming vectors, and the allocated power.
- Using both link-level and system-level simulations, we show the proposed precoding method significantly outperforms the existing linear precoding techniques including MRT, ZF, SLNR, M-MMSE, and the sum-spectral efficiency maximization precoding methods in both perfect and imperfect local CSIT cases. One remarkable observation is that the proposed method asymptotically achieves the ergodic spectral efficiency that attained under the no ICI scenario, i.e., (the single-cell upper bound). This result confirms that the proposed noncooperative precoding technique is sufficient to achieve high spectral efficiencies in HetNets, provided that both the IUI and the ICI leakage are eliminated by sharply using local CSIT.

II. SYSTEM MODEL

As illustrated in Fig. 1, we consider a noncooperative massive MIMO HetNet, which comprises of L BSs each equipped with N_ℓ antennas for $\ell \in \mathcal{L} \triangleq \{1, \dots, L\}$. The ℓ th

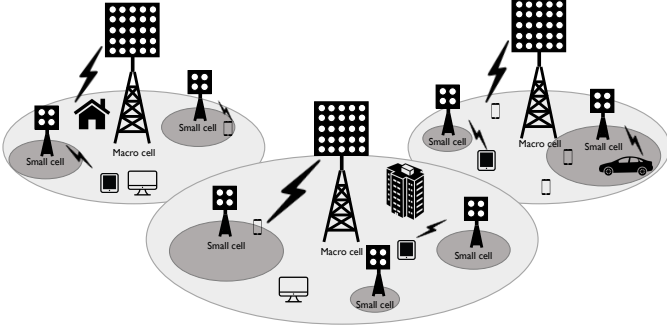


Fig. 1. An illustration of massive MIMO HetNets.

BS (possibly small/macro-cell BS) serves K_ℓ users with single antenna.

A. Downlink Channel Model

We denote the downlink channel vector from the j th BS to the k th user in the ℓ th cell by $\mathbf{h}_{j,\ell,k} \in \mathbb{C}^{N_j \times 1}$. This downlink channel is modeled as

$$\mathbf{h}_{j,\ell,k} = \beta_{j,\ell,k}^{\frac{1}{2}} \mathbf{g}_{j,\ell,k}, \quad (1)$$

where $\beta_{j,\ell,k} \in \mathbb{R}$ is a large scale fading coefficient and $\mathbf{g}_{j,\ell,k} \in \mathbb{C}^{N_j \times 1}$ is a small scale fading, which is distributed as $\mathbf{h}_{j,\ell,k} \sim \mathcal{CN}(0, \beta_{j,\ell,k} \mathbf{R}_{j,\ell,k})$ with $\mathbf{R}_{j,\ell,k} = \mathbb{E}[\mathbf{g}_{j,\ell,k} \mathbf{g}_{j,\ell,k}^H]$ for $\forall j, \ell \in \mathcal{L}$ and $\forall k \in \mathcal{K}_\ell \triangleq \{1, \dots, K_\ell\}$. This matrix captures the spatial correlation information on the channel. Under a stationary process assumption, it is typically obtained by using both angle-of-arrival (AoA) vectors of multipaths and the corresponding angular autocorrelation function.

B. Local CSIT Acquisition with Pilot Contamination Effect

Thanks to the channel reciprocity, in TDD massive MIMO HetNets, each BS is able to predict the downlink channel vectors for a set of users using uplink pilot sequences. Let $\mathbf{q}_{\ell,k} \in \mathbb{C}^{\tau \times 1}$ be the uplink pilot sequence with length τ sent by the k th user in the ℓ th cell. We assume that the users in the same cell use the orthogonal pilot sequences, i.e., $\mathbf{q}_{\ell,k}^H \mathbf{q}_{\ell,i} = 0$ for $i, k \in \mathcal{K}_\ell$. In addition, to mitigate both the pilot contamination effect and ICI, we assume that a set of users in the adjacent cells of the ℓ th cell also utilizes the orthogonal uplink pilot sequences. Specifically, we define a set of user indices in the adjacent cells of the ℓ th cell who use orthogonal uplink pilots with all users in the ℓ th cell by $\mathcal{U}_\ell = \{(j, i) : \mathbf{q}_{j,i}^H \mathbf{q}_{\ell,k} = 0\} \forall k \in \mathcal{K}_\ell$. Under these assumptions, the ℓ th BS is able to estimate both the downlink channel of the users in the own cell $\{\mathbf{h}_{\ell,\ell,1}, \mathbf{h}_{\ell,\ell,2}, \dots, \mathbf{h}_{\ell,\ell,K_\ell}\}$ and in the other cell users $\{\mathbf{h}_{j,\ell,i}\}$ where $(j, i) \in \mathcal{U}_\ell$. In a similar manner, each BS has knowledge of local CSIT, i.e., CSIT for all users in the own cell and partial users in the adjacent cells.

From the uplink pilots, each BS estimates the channel using the MMSE estimator. Let $\tilde{\mathbf{h}}_{\ell,\ell,k}$ be the estimated downlink channel. Then, it can be represented as the superposition of the true channel vector and an estimation error vector as

$$\tilde{\mathbf{h}}_{\ell,\ell,k} = \mathbf{h}_{\ell,\ell,k} - \mathbf{e}_{\ell,\ell,k}, \quad (2)$$

where $\mathbf{e}_{\ell,\ell,k}$ is the estimation error vector. This error vector is statistically independent of the estimate $\tilde{\mathbf{h}}_{\ell,\ell,k}$, and it follows the complex Gaussian distribution, i.e., $\mathcal{CN}(\mathbf{0}, \Phi_{\ell,\ell,k})$ where $\Phi_{\ell,\ell,k} = \mathbb{E}[\mathbf{e}_{\ell,\ell,k} \mathbf{e}_{\ell,\ell,k}^H] \in \mathbb{C}^{N_\ell \times N_\ell}$ is the error covariance matrix. The error covariance matrix $\Phi_{\ell,\ell,k}$ is a function of the pilot pattern, the length of pilot sequence τ , uplink pilot power p_{ul} , and channel covariance matrix $\mathbf{R}_{\ell,\ell,k}$. Let $\mathcal{C}_{\ell,k} = \{(j, i) | \mathbf{q}_{\ell,k}^H \mathbf{q}_{j,i} \neq 0\} \cup (\ell, k)$ be the set of users who use the non-orthogonal uplink pilots with that of the k th user in the ℓ th cell. Using this notation as shown in [29], [30], the error covariance matrix is computed as

$$\Phi_{\ell,\ell,k} = \beta_{\ell,\ell,k} \mathbf{R}_{\ell,\ell,k} - \beta_{\ell,\ell,k}^2 \mathbf{R}_{\ell,\ell,k} \left(\sum_{(j,i) \in \mathcal{C}_{\ell,k}} \beta_{\ell,j,i} \mathbf{R}_{\ell,j,i} + \frac{\sigma^2}{\tau p_{\text{ul}}} \mathbf{I}_N \right)^{-1} \mathbf{R}_{\ell,\ell,k}. \quad (3)$$

C. Downlink Spectral Efficiency with Local and Imperfect CSIT

Using imperfect and local CSIT at the ℓ th BS, i.e., $\{\tilde{\mathbf{h}}_{\ell,\ell,1}, \tilde{\mathbf{h}}_{\ell,\ell,2}, \dots, \tilde{\mathbf{h}}_{\ell,\ell,K_\ell}\}$ and $\{\tilde{\mathbf{h}}_{j,\ell,i}\}$ where $(j, i) \in \mathcal{U}_\ell$, it constructs the precoded data symbol vector $\mathbf{x}_\ell \in \mathbb{C}^{N_\ell \times 1}$ by a linear combination of precoding vectors $\mathbf{f}_{\ell,k}$ and data symbol $s_{\ell,k}$ as

$$\mathbf{x}_\ell = \sum_{k=1}^{K_\ell} \mathbf{f}_{\ell,k} s_{\ell,k}, \quad (4)$$

for $\forall \ell \in \mathcal{L}$ and $\forall k \in \mathcal{K}_\ell$. Assuming that data symbol $s_{\ell,k}$ is drawn from a Gaussian codebook with transmit power P_ℓ , i.e., $s_{\ell,k} \sim \mathcal{CN}(0, P_\ell)$, the linear precoding vectors should satisfy the sum power constraint of $\sum_{k=1}^{K_\ell} \|\mathbf{f}_{\ell,k}\|_2^2 \leq 1$. Then, the received signal of the k th user in the ℓ th cell is given by

$$\begin{aligned} y_{\ell,k} &= \sum_{j=1}^L \mathbf{h}_{j,\ell,k}^H \mathbf{x}_j + n_{\ell,k} \\ &= \mathbf{h}_{\ell,\ell,k}^H \mathbf{f}_{\ell,k} s_{\ell,k} + \sum_{i \neq k} \mathbf{h}_{\ell,\ell,k}^H \mathbf{f}_{\ell,i} s_{\ell,i} + \sum_{j \neq \ell} \sum_{i=1}^{K_j} \mathbf{h}_{j,\ell,k}^H \mathbf{f}_{j,i} s_{j,i} + n_{\ell,k}, \end{aligned} \quad (5)$$

where $n_{\ell,k}$ is the additive complex Gaussian noise with zero-mean and variance σ^2 , i.e., $\mathcal{CN}(0, \sigma^2)$. Then, the signal-to-interference-plus-noise ratio (SINR) of the k th user in the ℓ th cell is given by

$$\text{SINR}_{\ell,k} = \frac{|\mathbf{h}_{\ell,\ell,k}^H \mathbf{f}_{\ell,k}|^2}{\sum_{i \neq k} |\mathbf{h}_{\ell,\ell,k}^H \mathbf{f}_{\ell,i}|^2 + \sum_{i=1}^{K_j} \sum_{j \neq \ell} \frac{P_j}{P_\ell} |\mathbf{h}_{j,\ell,k}^H \mathbf{f}_{j,i}|^2 + \frac{\sigma^2}{P_\ell}}. \quad (6)$$

The instantaneous sum-spectral efficiency of the network is

$$\sum_{\ell=1}^L \sum_{k=1}^{K_\ell} R_{\ell,k} = \sum_{\ell=1}^L \sum_{k=1}^{K_\ell} \log_2(1 + \text{SINR}_{\ell,k}). \quad (7)$$

III. SILNR MAXIMIZATION PRECODING

In this section, we introduce a new performance metric, called SILNR. Then, we present the maximization problem for a lower bound of sum-spectral efficiency using SILNR.

A. SILNR with Local and Imperfect CSIT

Using imperfect and local CSIT at the ℓ th BS, the received signal of the k th user in the ℓ th cell is rewritten as

$$y_{\ell,k} = \tilde{\mathbf{h}}_{\ell,\ell,k}^H \mathbf{f}_{\ell,k} s_{\ell,k} + \sum_{i \neq k}^{K_\ell} \tilde{\mathbf{h}}_{\ell,\ell,k}^H \mathbf{f}_{\ell,i} s_{\ell,i} + \sum_{i=1}^{K_\ell} \mathbf{e}_{\ell,\ell,k}^H \mathbf{f}_{\ell,i} s_{\ell,i} + \tilde{n}_{\ell,k}, \quad (8)$$

where

- $\sum_{i \neq k}^{K_\ell} \tilde{\mathbf{h}}_{\ell,\ell,k}^H \mathbf{f}_{\ell,i} s_{\ell,i}$ denotes IUI,
- $\sum_{i=1}^{K_\ell} \mathbf{e}_{\ell,\ell,k}^H \mathbf{f}_{\ell,i} s_{\ell,i}$ is IUI caused by the channel estimation error,
- and $\tilde{n}_{\ell,k}$ is the effective noise when treating all aggregated ICI as additional noise.

In particular, this effective noise $\tilde{n}_{\ell,k}$ can be decompose into the uncontrollable ICI and controllable ICI by the other cell BSs, which have estimated the interfering channel from them to the k th user in the ℓ th cell. Let $\mathcal{L}_\ell = \{j : \mathbf{q}_{\ell,k}^H \mathbf{q}_{j,i} = 0, \forall i \in \mathcal{K}_j\}$ be the collection of the other cell BSs, in which all associated users use orthogonal pilots with the pilot of the k th user in the ℓ th cell.

$$\begin{aligned} \tilde{n}_{\ell,k} = & \sum_{j \in \mathcal{L}_\ell} \sum_{k=1}^{K_j} \tilde{\mathbf{h}}_{j,\ell,k}^H \mathbf{f}_{j,k} s_{j,k} + \sum_{j \in \mathcal{L}_\ell} \sum_{k=1}^{K_j} \mathbf{e}_{j,\ell,k}^H \mathbf{f}_{j,k} s_{j,k} \\ & + \sum_{j \notin \mathcal{L}_\ell} \sum_{k=1}^{K_j} \mathbf{h}_{j,\ell,k}^H \mathbf{f}_{j,k} s_{j,k} + n_{\ell,k}. \end{aligned} \quad (9)$$

Ideally, $\sum_{j \in \mathcal{L}_\ell} \sum_{k=1}^{K_j} \tilde{\mathbf{h}}_{j,\ell,k}^H \mathbf{f}_{j,k} s_{j,k}$ can be eliminated by the other BSs, provided that they perform ICI nulling precoding using their local CSIT. In addition, we also define the aggregated leakage interference towards the other cell users by the transmission of the k th user in the ℓ th cell. This leakage interference $\mathcal{L}_{\ell,k}$ is

$$\mathcal{L}_{\ell,k} = \mathbf{f}_{\ell,k}^H \left(\sum_{\substack{j \in \mathcal{L}_\ell \\ i \in \mathcal{K}_j}} \tilde{\mathbf{h}}_{j,\ell,i} \tilde{\mathbf{h}}_{\ell,j,i}^H \right) \mathbf{f}_{\ell,k}. \quad (10)$$

Incorporating (8), (9), and (10), we define SILNR of the k th user in the ℓ th cell as

$$\text{SILNR}_{\ell,k} = \frac{\left| \tilde{\mathbf{h}}_{\ell,\ell,k}^H \mathbf{f}_{\ell,k} \right|^2}{\sum_{i \neq k}^{K_\ell} \left| \tilde{\mathbf{h}}_{\ell,\ell,k}^H \mathbf{f}_{\ell,i} \right|^2 + \sum_{i=1}^{K_\ell} \mathbf{f}_{\ell,i}^H \Phi_{\ell,\ell,k} \mathbf{f}_{\ell,i} + \mathcal{L}_{\ell,k} + \frac{\tilde{\sigma}_{\ell,k}^2}{P}}. \quad (11)$$

We provide some remarks on this SILNR value.

Remark 1 (Connection to achievable spectral efficiencies): The SILNR defined in (11) is always smaller than SINR,

because the leakage power is positive. Therefore, one can interpret

$$\log_2 (1 + \text{SILNR}_{\ell,k}) \quad (12)$$

as a lower bound of the spectral efficiency of $\log_2 (1 + \text{SINR}_{\ell,k})$ by penalizing the interference leakage generated by the transmission of data symbol $s_{\ell,k}$ to the other cells. If we ignore this interference leakage power $\mathcal{L}_{\ell,k}$, $\log_2 (1 + \text{SINR}_{\ell,k})$ is a well-known lower bound of the downlink spectral efficiency derived by the generalized mutual information (GMI) [31]–[34], in which the non-Gaussian IUI term caused by the channel estimation error $\sum_{i=1}^{K_\ell} \mathbf{e}_{\ell,\ell,k}^H \mathbf{f}_{\ell,i} s_{\ell,i}$ is treated as the Gaussian noise with the variance matching.

In addition, the spectral efficiency in (12) is achievable when each downlink user can perfectly estimate the precoded channel $\tilde{\mathbf{h}}_{\ell,\ell,k}^H \mathbf{f}_{\ell,k}$. This precoded channel estimation can be accurately performed by demodulation reference signals currently used in LTE systems [35]. One can also readily incorporate the error effect in estimating $\tilde{\mathbf{h}}_{\ell,\ell,k}^H \mathbf{f}_{\ell,k}$ using the concept of GMI. We ignore this estimation error effect of the precoded channel for ease of exposition.

Remark 2 (Difference with prior work): Our SILNR definition in (11) differs from the definition of SILNR used in some prior works [36], [37], in which the IUI power received by other users' transmission $\sum_{i \neq k}^{K_\ell} \left| \tilde{\mathbf{h}}_{\ell,\ell,k}^H \mathbf{f}_{\ell,i} \right|^2$ was not incorporated. Instead, the IUI term is modeled as an additional intra-cell interference leakage power, i.e., $\sum_{i \neq k}^{K_\ell} \left| \tilde{\mathbf{h}}_{\ell,i,k}^H \mathbf{f}_{\ell,k} \right|^2$. Although the terminology of SILNR was initially introduced in [36], [37], this SILNR definition is equivalent to SLNR [21] in a multicell setting, as the authors mentioned. In addition, the definition of in SILNR was interchangeably used with the SLNR [36], [37]. We use our definition of SILNR in the sequel.

B. SILNR Maximization

We consider an optimization problem that maximizes the lower bound of the sum-spectral efficiency in the ℓ th cell using local CSIT under the per-BS power constraint:

$$\arg \max_{\mathbf{f}_{\ell,1}, \dots, \mathbf{f}_{\ell,K_\ell}} \sum_{k=1}^{K_\ell} \log_2 (1 + \text{SILNR}_{\ell,k}), \quad (13)$$

$$\text{subject to } \sum_{i=1}^{K_\ell} \|\mathbf{f}_{\ell,i}\|_2^2 \leq 1, \quad \forall \ell \in \mathcal{L}. \quad (14)$$

To provide the intuition behind on the optimization problem defined in (13), it is instructive to compare it with the existing optimization problems for the precoding design.

Case 1: One is the case when the leakage term in (11) is discarded. In this case, the problem (13) boils down to the

sum-spectral efficiency maximization problem as in our prior work [27], [28], i.e.,

$$\arg \max_{\mathbf{f}_{\ell,1}, \dots, \mathbf{f}_{\ell,K_\ell}} \sum_{k=1}^{K_\ell} \log_2 (1 + \text{SINR}_{\ell,k}), \quad (15)$$

$$\text{subject to } \sum_{i=1}^{K_\ell} \|\mathbf{f}_{\ell,i}\|_2^2 \leq 1, \quad \forall \ell \in \mathcal{L}. \quad (16)$$

Case 2: The other case is when the IUI power term is ignored in SILNR (11). In this case, our optimization problem (13) becomes the SLNR maximization problem per $\mathbf{f}_{\ell,k}$ in a multicell setting [21], i.e.,

$$\arg \max_{\mathbf{f}_{\ell,k}} \frac{|\tilde{\mathbf{h}}_{\ell,\ell,k}^H \mathbf{f}_{\ell,k}|^2}{\mathbf{f}_{\ell,k}^H \left(\sum_{j \in \mathcal{L}_\ell} \tilde{\mathbf{h}}_{\ell,j,i} \tilde{\mathbf{h}}_{\ell,j,i}^H + \frac{\tilde{\sigma}_{\ell,k}^2}{P_{\ell,k}} \mathbf{I} \right) \mathbf{f}_{\ell,k}}, \quad (17)$$

for $k \in \{1, 2, \dots, K_\ell\}$. The optimal solution for this problem is obtained in a closed-form by finding the maximum eigenvector of $\left(\sum_{j \in \mathcal{L}_\ell} \tilde{\mathbf{h}}_{\ell,j,i} \tilde{\mathbf{h}}_{\ell,j,i}^H + \frac{\tilde{\sigma}_{\ell,k}^2}{P_{\ell,k}} \mathbf{I} \right)^{-1} \left(\tilde{\mathbf{h}}_{\ell,\ell,k} \tilde{\mathbf{h}}_{\ell,\ell,k}^H \right)$.

Case 3: When the IUI power is replaced by the intra-cell leakage power as in [36], [37], the multi-cell SLNR maximization precoding solution is obtained by solving the following optimization problem

$$\arg \max_{\mathbf{f}_{\ell,k}} \frac{|\tilde{\mathbf{h}}_{\ell,\ell,k}^H \mathbf{f}_{\ell,k}|^2}{\mathbf{f}_{\ell,k}^H \left(\sum_{i \neq k}^{K_\ell} \tilde{\mathbf{h}}_{\ell,i,k} \tilde{\mathbf{h}}_{\ell,i,k}^H + \sum_{j \in \mathcal{L}_\ell} \tilde{\mathbf{h}}_{\ell,j,i} \tilde{\mathbf{h}}_{\ell,j,i}^H + \frac{\tilde{\sigma}_{\ell,k}^2}{P_{\ell,k}} \mathbf{I} \right) \mathbf{f}_{\ell,k}}, \quad (18)$$

for $k \in \{1, 2, \dots, K_\ell\}$. Similarly, the optimal solution is the maximum eigenvector of

$$\left(\sum_{i \neq k}^{K_\ell} \tilde{\mathbf{h}}_{\ell,i,k} \tilde{\mathbf{h}}_{\ell,i,k}^H + \sum_{j \in \mathcal{L}_\ell} \tilde{\mathbf{h}}_{\ell,j,i} \tilde{\mathbf{h}}_{\ell,j,i}^H + \frac{\tilde{\sigma}_{\ell,k}^2}{P_{\ell,k}} \mathbf{I} \right)^{-1} \left(\tilde{\mathbf{h}}_{\ell,\ell,k} \tilde{\mathbf{h}}_{\ell,\ell,k}^H \right).$$

This solution is also equivalent to the uplink multi-cell MMSE (M-MMSE) precoding method inspired by the uplink-downlink duality [23]. This M-MMSE precoding method, however, does not necessarily maximize the downlink sum spectral efficiencies.

C. Reformulation

We reformulate (13) into the maximization problem of the product of the Rayleigh quotients by lifting all optimization variables in a large-dimensional space. To accomplish this, by aggregating all precoding vectors used at the ℓ th cell, we first define a large dimensional precoding vector $\mathbf{f}_\ell \in \mathbb{C}^{N_\ell K_\ell} \times 1$ as

$$\mathbf{f}_\ell = \left[\mathbf{f}_{\ell,1}^H, \dots, \mathbf{f}_{\ell,k}^H, \dots, \mathbf{f}_{\ell,K_\ell}^H \right]^H, \quad \forall \ell \in \mathcal{L}. \quad (19)$$

The signal and the aggregated interference power terms of SILNR defined in (11) can be written as a quadratic function with respective to \mathbf{f}_ℓ as

$$\sum_{i=1}^{K_\ell} |\tilde{\mathbf{h}}_{\ell,\ell,k}^H \mathbf{f}_{\ell,i}|^2 + \sum_{i=1}^{K_\ell} \mathbf{f}_{\ell,i}^H \Phi_{\ell,\ell,k} \mathbf{f}_{\ell,i} + \mathbf{L}_{\ell,k} + \frac{\tilde{\sigma}_{\ell,k}^2}{P} = \mathbf{f}_\ell^H \mathbf{A}_{\ell,k} \mathbf{f}_\ell, \quad (20)$$

$$\sum_{i \neq k}^{K_\ell} |\tilde{\mathbf{h}}_{\ell,\ell,k}^H \mathbf{f}_{\ell,i}|^2 + \sum_{i=1}^{K_\ell} \mathbf{f}_{\ell,i}^H \Phi_{\ell,\ell,k} \mathbf{f}_{\ell,i} + \mathbf{L}_{\ell,k} + \frac{\tilde{\sigma}_{\ell,k}^2}{P} = \mathbf{f}_\ell^H \mathbf{B}_{\ell,k} \mathbf{f}_\ell, \quad (21)$$

where $\mathbf{A}_{\ell,k}$ and $\mathbf{B}_{\ell,k}$ are defined as

$$\mathbf{A}_{\ell,k} = \text{diag} \left(\tilde{\mathbf{h}}_{\ell,\ell,k} \tilde{\mathbf{h}}_{\ell,\ell,k}^H + \Phi_{\ell,\ell,k}, \dots, \tilde{\mathbf{h}}_{\ell,\ell,k} \tilde{\mathbf{h}}_{\ell,\ell,k}^H + \Phi_{\ell,\ell,k} \right) + \text{diag} \left(\mathbf{0}, \dots, \mathbf{L}_{\ell,k}, \dots, \mathbf{0} \right) + \tilde{\sigma}_{\ell,k}^2 / P \mathbf{I}_{N_\ell}, \quad (22)$$

$$\mathbf{B}_{\ell,k} = \mathbf{A}_{\ell,k} - \text{diag} \left(\mathbf{0}, \dots, \tilde{\mathbf{h}}_{\ell,\ell,k} \tilde{\mathbf{h}}_{\ell,\ell,k}^H, \dots, \mathbf{0} \right). \quad (23)$$

Using these, the SILNR of the k th user in the ℓ th cell is represented as a ratio of the two quadratic functions with respective to the aggregated precoding vector $\mathbf{f}_\ell \in \mathbb{C}^{N_\ell K_\ell}$ as

$$\text{SILNR}_{\ell,k} = \frac{\mathbf{f}_\ell^H \mathbf{A}_{\ell,k} \mathbf{f}_\ell}{\mathbf{f}_\ell^H \mathbf{B}_{\ell,k} \mathbf{f}_\ell}. \quad (24)$$

As a result, the optimization problem in (13)-(14) is equivalent to the maximization problem of the product of Rayleigh quotients, namely,

$$\arg \max_{\mathbf{f}_\ell \in \mathbb{C}^{N_\ell K_\ell}} \prod_{k=1}^{K_\ell} \frac{\mathbf{f}_\ell^H \mathbf{A}_{\ell,k} \mathbf{f}_\ell}{\mathbf{f}_\ell^H \mathbf{B}_{\ell,k} \mathbf{f}_\ell}, \quad (25)$$

$$\text{subject to } \|\mathbf{f}_\ell\|_2^2 = 1, \quad \forall \ell \in \mathcal{L}. \quad (26)$$

Let $\gamma(\mathbf{f}_\ell) = \prod_{k=1}^{K_\ell} \frac{\mathbf{f}_\ell^H \mathbf{A}_{\ell,k} \mathbf{f}_\ell}{\mathbf{f}_\ell^H \mathbf{B}_{\ell,k} \mathbf{f}_\ell}$ be the non-convex objective function. Notice that this objective function is invariant to any positive scale of \mathbf{f}_ℓ . This property allows us to ignore the sum-power constraint in (26) when solving the non-convex optimization problem. Hence, we focus on the following unconstrained non-convex optimization problem:

$$\arg \max_{\mathbf{f}_\ell \in \mathbb{C}^{N_\ell K_\ell}} \prod_{k=1}^{K_\ell} \frac{\mathbf{f}_\ell^H \mathbf{A}_{\ell,k} \mathbf{f}_\ell}{\mathbf{f}_\ell^H \mathbf{B}_{\ell,k} \mathbf{f}_\ell}. \quad (27)$$

The finding the optimal solution for the non-convex optimization problem in (27) is a very challenging task. In the sequel, we introduce an algorithm to find a local optimal solution of this non-convex optimization problem.

IV. LOCAL OPTIMALITY CONDITIONS

In this section, we derive the first- and the second-order necessary conditions for the local optimality of the non-convex optimization problem in (13).

The following theorems are the main results of this section.

Theorem 1. (The first-order necessary condition) If $\mathbf{f}_\ell^* \in \mathbb{C}^{N_\ell K_\ell \times 1}$ is a local optimal solution of the non-convex optimization problem (27), it satisfies

$$\bar{\mathbf{A}}_\ell(\mathbf{f}_\ell^*) \mathbf{f}_\ell^* = \gamma(\mathbf{f}_\ell^*) \bar{\mathbf{B}}_\ell(\mathbf{f}_\ell^*) \mathbf{f}_\ell^*, \quad (28)$$

where the functional matrices $\bar{\mathbf{A}}_\ell(\mathbf{f}_\ell^*)$ and $\bar{\mathbf{B}}_\ell(\mathbf{f}_\ell^*)$ are

$$\begin{aligned}\bar{\mathbf{A}}_\ell(\mathbf{f}_\ell^*) &= \prod_{k=1}^{K_\ell} \left((\mathbf{f}_\ell^*)^H \mathbf{A}_{\ell,k} \mathbf{f}_\ell^* \right) \sum_{i=1}^{K_\ell} \frac{\mathbf{A}_{\ell,i}}{(\mathbf{f}_\ell^*)^H \mathbf{A}_{\ell,i} \mathbf{f}_\ell^*}, \\ \bar{\mathbf{B}}_\ell(\mathbf{f}_\ell^*) &= \prod_{k=1}^{K_\ell} \left((\mathbf{f}_\ell^*)^H \mathbf{B}_{\ell,k} \mathbf{f}_\ell^* \right) \sum_{i=1}^{K_\ell} \frac{\mathbf{B}_{\ell,i}}{(\mathbf{f}_\ell^*)^H \mathbf{B}_{\ell,i} \mathbf{f}_\ell^*}.\end{aligned}\quad (29)$$

Proof: The proof is analogous in the companion paper [28]. For the completeness, we provide the proof in Appendix A. ■

Theorem 1 implies that any saddle point of the non-convex problem in (27) is one of the eigenvectors of the functional matrix $[\bar{\mathbf{B}}_\ell(\mathbf{f}_\ell)]^{-1} \bar{\mathbf{A}}_\ell$, i.e.,

$$[\bar{\mathbf{B}}_\ell(\mathbf{f}_\ell)]^{-1} \bar{\mathbf{A}}_\ell(\mathbf{f}_\ell) \mathbf{f}_\ell = \gamma(\mathbf{f}_\ell) \mathbf{f}_\ell. \quad (30)$$

As can be seen, the objective function $\gamma(\mathbf{f}_\ell)$ can be interpreted as the eigenvalue of the functional matrix $[\bar{\mathbf{B}}_\ell(\mathbf{f}_\ell)]^{-1} \bar{\mathbf{A}}_\ell$. Since we are interested in maximizing the objective function $\gamma(\mathbf{f}_\ell)$, we need to identify the eigenvector corresponding to the maximum eigenvalue, which can be a global optimal solution. Unfortunately, finding such eigenvector is highly non-trivial, because $[\bar{\mathbf{B}}_\ell(\mathbf{f}_\ell)]^{-1} \bar{\mathbf{A}}_\ell$ is a function of \mathbf{f}_ℓ . Nevertheless, this eigensystem analysis helps to understand the global landscape of the non-convex optimization problem; and leads to an algorithm to find a local optimal solution in a numerical manner.

Although \mathbf{f}_ℓ^* satisfies the first-order necessary condition derived in Theorem 1, we need to check the curvature of the objective function around the stationary point to verify the local optimality. The following theorem gives a testing condition of the negative definiteness of the Hessian matrix evaluated at \mathbf{f}_ℓ^* in a closed-form, i.e., $\nabla_{\mathbf{f}}^2 \gamma(\mathbf{f}_\ell^*) < 0$.

Theorem 2. (The second-order necessary condition) *The stationary point \mathbf{f}_ℓ^* is a local-optimal solution, provided that*

$$\rho_{\min} \left(\sum_{i=1}^{K_\ell} \frac{\mathbf{A}_{\ell,i}^H \mathbf{f}_\ell^* (\mathbf{f}_\ell^*)^H \mathbf{A}_{\ell,i}}{\left((\mathbf{f}_\ell^*)^H \mathbf{A}_{\ell,i} \mathbf{f}_\ell^* \right)^2} \right) > \rho_{\max} \left(\sum_{i=1}^{K_\ell} \frac{\mathbf{B}_{\ell,i}^H \mathbf{f}_\ell^* (\mathbf{f}_\ell^*)^H \mathbf{B}_{\ell,i}}{\left((\mathbf{f}_\ell^*)^H \mathbf{B}_{\ell,i} \mathbf{f}_\ell^* \right)^2} \right), \quad (31)$$

where $\rho_{\min}(\mathbf{Q})$ and $\rho_{\max}(\mathbf{Q})$ are the minimum and maximum eigenvalues of a matrix \mathbf{Q} .

Proof: See Appendix B. ■

We provide a useful interpretation of the testing condition in Theorem 2. Recall that $\sum_{i=1}^{K_\ell} \frac{\mathbf{A}_{\ell,i}^H \mathbf{f}_\ell^* (\mathbf{f}_\ell^*)^H \mathbf{A}_{\ell,i}}{\left((\mathbf{f}_\ell^*)^H \mathbf{A}_{\ell,i} \mathbf{f}_\ell^* \right)^2}$ in LHS of (31) is the sum of the covariance matrices that contain both the desired and interference power evaluated at \mathbf{f}_ℓ^* . Whereas, $\sum_{i=1}^{K_\ell} \frac{\mathbf{B}_{\ell,i}^H \mathbf{f}_\ell^* (\mathbf{f}_\ell^*)^H \mathbf{B}_{\ell,i}}{\left((\mathbf{f}_\ell^*)^H \mathbf{B}_{\ell,i} \mathbf{f}_\ell^* \right)^2}$ in RHS of (31) is the sum of the covariance matrices that only consist of the interference power evaluated at \mathbf{f}_ℓ^* . To be a local optimal solution, it is sufficient to check whether the maximum possible interference power is less than

the minimum of the aggregated received power. This closed-form testing condition allows us to check the second-order optimality condition without directly computing the Hessian matrix $\nabla_{\mathbf{f}}^2 \gamma(\mathbf{f}_\ell^*)$.

V. SILNR MAXIMIZATION PRECODING

In this section, we present SILNR maximization precoding for massive MIMO HetNets. The key idea of the proposed algorithm is to find the maximum eigenvector of the functional matrix $[\bar{\mathbf{B}}_\ell(\mathbf{f}_\ell)]^{-1} \bar{\mathbf{A}}_\ell$. As shown in Theorem 1, the maximum eigenvector of $[\bar{\mathbf{B}}_\ell(\mathbf{f}_\ell)]^{-1} \bar{\mathbf{A}}_\ell$ is a stationary point. Therefore, to verify the local optimality, the proposed algorithm also uses the testing condition derived in Theorem 2.

The proposed algorithm consists of two steps: 1) the identification of a stationary point using the generalized power iteration (GPI) method in [28] and 2) the local-optimality validation. First of all, the SILNR maximization precoding initializes the algorithmic parameter including local-optimality-check (LOC) value to logical 0. Specifically, in the t th iteration, we calculate the functional matrices $\bar{\mathbf{A}}_\ell(\mathbf{f}_\ell^{(t-1)})$ and $\bar{\mathbf{B}}_\ell(\mathbf{f}_\ell^{(t-1)})$ defined in (29) using the previously found precoding vector $\mathbf{f}_\ell^{(t-1)}$. Then, it is multiplied with $[\bar{\mathbf{B}}_\ell(\mathbf{f}_\ell^{(t-1)})]^{-1} \bar{\mathbf{A}}_\ell(\mathbf{f}_\ell^{(t-1)})$ to obtain $\mathbf{f}_\ell^{(t)} = [\bar{\mathbf{B}}_\ell(\mathbf{f}_\ell^{(t-1)})]^{-1} \bar{\mathbf{A}}_\ell(\mathbf{f}_\ell^{(t-1)}) \mathbf{f}_\ell^{(t-1)}$. Then, the normalization of $\mathbf{f}_\ell^{(t)}$ is performed. These iterations continues until a stopping condition $\|\mathbf{f}_\ell^{(t-1)} - \mathbf{f}_\ell^{(t)}\|_2 \leq \epsilon$ is satisfied, where ϵ is selected as a small positive number. Once the eigenvector that satisfies the first-order necessary condition in Theorem 1 is identified, the proposed algorithm checks the local optimality by computing the eigenvalues of $\sum_{i=1}^{K_\ell} \frac{\mathbf{A}_{\ell,i}^H \mathbf{f}_\ell^* (\mathbf{f}_\ell^*)^H \mathbf{A}_{\ell,i}}{\left((\mathbf{f}_\ell^*)^H \mathbf{A}_{\ell,i} \mathbf{f}_\ell^* \right)^2}$ and $\sum_{i=1}^{K_\ell} \frac{\mathbf{B}_{\ell,i}^H \mathbf{f}_\ell^* (\mathbf{f}_\ell^*)^H \mathbf{B}_{\ell,i}}{\left((\mathbf{f}_\ell^*)^H \mathbf{B}_{\ell,i} \mathbf{f}_\ell^* \right)^2}$ by leveraging Theorem 2. If this testing condition is satisfied, the algorithm stops. Otherwise, it starts with a new initial point and finds a new eigenvector of the functional matrix. The proposed algorithm is summarized in Algorithm 1.

Remark 3 (The computational complexity of the algorithm): The computational complexity order of the proposed SILNR maximization precoding algorithm is $O(JN_\ell^2 K_\ell)$, where J is the number of iterations required to convergence about Theorem 1, i.e., $\|\gamma(\mathbf{f}_\ell^{(t-1)}) - \gamma(\mathbf{f}_\ell^{(t)})\|_2 \geq \epsilon$ for Algorithm 1. We refer the details of the computational complexity analysis in [28], in which the matrix inverse and the multiplication operations have shown to be performed in a divide and conquer manner by exploiting the block diagonal structure in $\bar{\mathbf{A}}_{\ell,k}$ and $\bar{\mathbf{B}}_{\ell,k}$. In addition, for the convergence, a number of iterations J is five at most in an average sense with respect to the locations of users. This claim will be numerically verified in Section V. The main reason behind on the fast convergence speed is because the ZF precoding solution is a sufficiently good initial solution when $N \gg K$ thanks to the channel hardening effects [10], [38]. This fast convergence property will be verified by numerical simulations in the sequel.

Algorithm 1: SILNR Maximization Precoding

Initialization:

 $t = j = \text{LOC} = 0$, $\mathbf{f}_\ell^{(0)} = \mathbf{Z}\mathbf{F}$, $\mathbf{f}_\ell^{(-1)} = \mathbf{0}$, and ϵ **while** $\text{LOC} == 0$ **do** $j \leftarrow j + 1$ **while** $\|\gamma(\mathbf{f}_\ell^{(t-1)}) - \gamma(\mathbf{f}_\ell^{(t)})\|_2 \geq \epsilon$ **do** $t \leftarrow t + 1$ $\mathbf{f}_\ell^{(t)} \leftarrow [\bar{\mathbf{B}}_\ell(\mathbf{f}_\ell^{(t-1)})]^{-1} \bar{\mathbf{A}}_\ell(\mathbf{f}_\ell^{(t-1)}) \mathbf{f}_\ell^{(t-1)}$ $\mathbf{f}_\ell^{(t)} \leftarrow \frac{\mathbf{f}_\ell^{(t)}}{\|\mathbf{f}_\ell^{(t)}\|_2}$ **end** **if** $j == 1$ **then** $\gamma^* \leftarrow \gamma(\mathbf{f}_\ell^{(t)})$ **end** **if** *Theorem 2 holds* **then** **if** $\gamma(\mathbf{f}_\ell^{(t)}) \geq \gamma^*$ **then** Return $\mathbf{f}_\ell^{(t)}$ **end** **else** $\text{LOC} \leftarrow 0$ $t \leftarrow 0$ $\mathbf{f}_\ell^{(0)} \leftarrow$ random unit vector **end****end**

We provide an example that captures the key difference between the proposed algorithm and the conventional sum-spectral efficiency maximization precoding method.

Example 1: We focus on the ℓ th cell, in which the BS equipped with four antennas $N_\ell = 4$ serves four downlink users, each with a single antenna. We also consider one user located at the j th cell location. In particular, we assume that the downlink channel vectors from the ℓ th cell to the k th user in the ℓ th cell and the i th user in the j th cell as

$$\begin{aligned} \mathbf{h}_{\ell,\ell,1} &= \begin{bmatrix} -0.8167 + 0.3869i \\ 0.08540 + 0.2124i \\ -0.0684 + 0.3500i \\ -0.0360 - 0.0475i \end{bmatrix}, \mathbf{h}_{\ell,\ell,2} = \begin{bmatrix} -0.1509 - 0.0932i \\ -0.7912 - 0.2040i \\ 0.37153 + 0.1498i \\ 0.32089 + 0.2035i \end{bmatrix}, \\ \mathbf{h}_{\ell,\ell,3} &= \begin{bmatrix} -0.4187 - 0.0786i \\ 0.8673 + 0.0134i \\ -0.0789 + 0.0021i \\ 0.0832 - 0.2298i \end{bmatrix}, \mathbf{h}_{\ell,\ell,4} = \begin{bmatrix} -0.2507 - 0.0280i \\ -0.0777 + 0.0137i \\ 0.9534 + 0.0047i \\ 0.0390 - 0.1394i \end{bmatrix}. \end{aligned} \quad (32)$$

In particular, we assume that channel vectors $\mathbf{h}_{\ell,\ell,3}$ and $\mathbf{h}_{\ell,\ell,4}$ are orthogonal, i.e., $\mathbf{h}_{\ell,\ell,3}^H \cdot \mathbf{h}_{\ell,\ell,4} = 0$. Whereas, the channel direction of user 4 is identical to that of the other cell user, i.e., $\mathbf{h}_{\ell,\ell,4} = 0.95\mathbf{h}_{\ell,j,i}$. In this simple setting, using the GPI algorithm in [27], [28], we obtain a joint user-selection, precoding, and power control solution for the sum-spectral

efficiency maximization problem:

$$\arg \max_{\mathbf{f}_{\ell,1}, \dots, \mathbf{f}_{\ell,4}} \sum_{k=1}^4 \log_2 (1 + \text{SINR}_{\ell,k}), \quad (33)$$

$$\text{subject to } \sum_{i=1}^4 \|\mathbf{f}_{\ell,i}\|_2^2 \leq 1, \quad \forall \ell \in \mathcal{L}. \quad (34)$$

The norms of the precoding vectors obtained from the algorithm are

$$\begin{bmatrix} \|\mathbf{f}_{1,1}\|_2^2 \\ \|\mathbf{f}_{1,2}\|_2^2 \\ \|\mathbf{f}_{1,3}\|_2^2 \\ \|\mathbf{f}_{1,4}\|_2^2 \end{bmatrix} = \begin{bmatrix} 0.2953 \\ 6.18 \cdot 10^{-5} \\ 0.3604 \\ 0.3442 \end{bmatrix}. \quad (35)$$

This result implies that the joint transmission for user 1, 3, and 4 is beneficial to maximize the sum-spectral efficiency. In contrast to the sum-spectral efficiency maximization precoding, the proposed SILNR maximization precoding solution is obtained by solving the following optimization problem:

$$\arg \max_{\mathbf{f}_{\ell,1}, \dots, \mathbf{f}_{\ell,4}} \sum_{k=1}^4 \log_2 (1 + \text{SILNR}_{\ell,k}), \quad (36)$$

$$\text{subject to } \sum_{i=1}^4 \|\mathbf{f}_{\ell,i}\|_2^2 \leq 1, \quad \forall \ell \in \mathcal{L}. \quad (37)$$

When applying the algorithm in Algorithm 1, one can obtain the norms of the precoding vectors as

$$\begin{bmatrix} \|\mathbf{f}_{1,1}\|_2^2 \\ \|\mathbf{f}_{1,2}\|_2^2 \\ \|\mathbf{f}_{1,3}\|_2^2 \\ \|\mathbf{f}_{1,4}\|_2^2 \end{bmatrix} = \begin{bmatrix} 0.4461 \\ 0.0015 \\ 0.4538 \\ 0.0985 \end{bmatrix}. \quad (38)$$

As can be seen, when taking into account the other-cell user, the SILNR maximization precoding solution is to serve both user 1 and 3. This result differs from the solution in (35), because user 4 is not served even if the channel vectors $\mathbf{h}_{\ell,\ell,3}$ and $\mathbf{h}_{\ell,\ell,4}$ are orthogonal, i.e., $\mathbf{h}_{\ell,\ell,3}^H \cdot \mathbf{h}_{\ell,\ell,4} = 0$. This example clearly elucidates the difference between the SILNR and the sum spectrum efficiency maximization precoding solutions.

VI. SIMULATION RESULTS

In this section, we provide both link level and system level simulation results to gauge the performance gains of the proposed SILNR maximization precoding method compared to the existing precoding methods.

A. Link Level Simulations

We consider a two-cell scenario in which each BS equipped with $N_\ell \in \{16, 32\}$ serves single antenna eight users who are located at the cell-edge. This channel model is also known as a two-cell (symmetric) interfering broadcast channel [39]. For link level simulations, we assume that all channel vectors are drawn from $\mathbf{h}_{j,\ell,k} \sim \mathcal{CN}(0, \mathbf{I})$, and each BS has perfect knowledge of local CSIT. In this setting, we compare the ergodic sum-spectral efficiency for different precoding strategies:

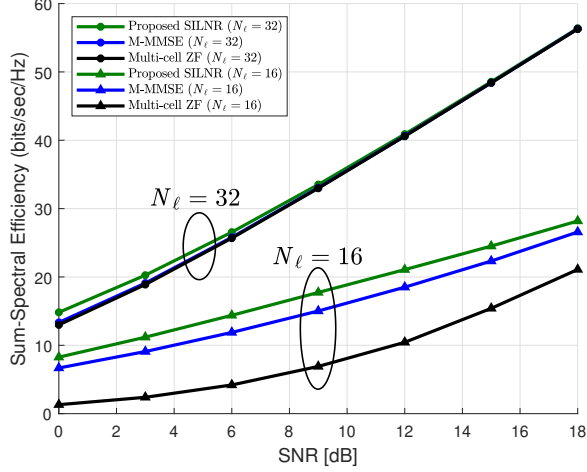


Fig. 2. The ergodic sum-spectral efficiency comparisons for different precoding strategies using local CSIT.

- MRT [14]: this scheme is the simple conjugate beamforming.
- Multi-cell ZF precoding [17]: this strategy removes both IUI and the interference leakage towards the other-cell users.
- M-MMSE (or multi-cell SLNR) precoding [21]: This scheme uses the downlink precoding solution in (18) by the uplink-downlink duality [22]–[24]. This scheme also maximizes the ratio between the desired signal power and the aggregated IUI and ICI interference leakage power in the multicell setting [23].
- SumRate-Max precoding [27], [28]: this method maximizes the sum-spectral efficiency per cell by finding a joint solution for user selection, precoding, and power allocation in multi-cell MU-MIMO systems.

Fig. 2 shows how the ergodic sum-spectral efficiency changes when increasing SNRs for different precoding strategies. When the number of antennas per each BS is 16, the proposed SILNR maximization precoding yields considerable gains compared to the existing precoding methods in all SNRs. The gain mainly stems from better utilization of spatial degrees of freedom to mitigate both IUI and ICI. For example, each precoding vector for the multicell ZF precoding should be in the null space of the column space spanned by the interfering channel vectors. This method may significantly decrease the desired signal power for each user. Unlike this method, the proposed SILNR jointly finds a set of served users, precoding vectors, and power. Therefore, it allows for each BS to exploit the spatial degrees of freedom in a more efficient way to increase the sum-spectral efficiency of the cell, while simultaneously reducing interference leakage power towards the other cell users. Whereas, when $N_t/K_t = 4$, all precoding methods achieve the similar sum-spectral efficiency in high SNRs because of the channel hardening effects [10], [38]. This fact implies that when the number of antennas at the BS is sufficiently large, the simple precoding is sufficient as reported in [10].

TABLE I
SYSTEM LEVEL SIMULATION ASSUMPTIONS.

Parameters	Value
Topology of BS	Irregular 19 hexagonal cells
Topology of user	Randomly distributed
Bandwidth	20 MHz
Carrier frequency	2 GHz
Macro BS transmission power	46 dBm
Pico BS transmission power	23 dBm
Noise power	-113 dB
Spatial channel model	Spatially correlated model
Path-loss model	Okumura-Hata model
BS and user height	32 m/1.5 m
Channel estimation	Imperfect

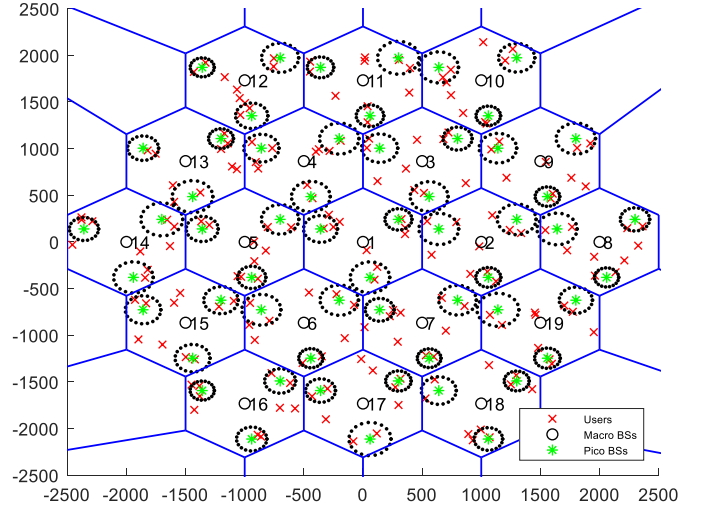


Fig. 3. An illustration for the network topologies used in system-level simulations.

B. System Level Simulations

For system level simulations, as depicted in Fig. 3, we consider the hexagonal-cell topology, in which each cell consists of one macro BS and three pico BSs. Each pico BS equipped with N antennas serves two users who are uniformly distributed in the dotted line circle, called the hotspot area. Meanwhile, each macro BS equipped with $5N$ antennas serves four users who are uniformly distributed in the hexagonal cell except the hotspot areas covered by the three pico cells. In addition, the macro and pico BS use the transmission power of 46 dBm and 23 dBm, respectively. The other simulation parameters for the massive MIMO HetNet are summarized in Table I.

Ergodic sum-spectral efficiency performance: We evaluate how the ergodic sum-spectral efficiency alters when increasing the number of antennas of both macro and pico BSs. In this simulation, we set the number of pico BS antennas to 20% of those of the macro BS. We consider two scenarios of local CSIT. One is the case when the ten users per the hexagonal cell area use orthogonal uplink pilots. Another case is when 70 uplink users in the area of seven hexagonal cells employ the orthogonal pilots. We compare the proposed precoding methods with the conventional MRT, ZF, and M-MMSE precoding methods using local CSIT. In addition,

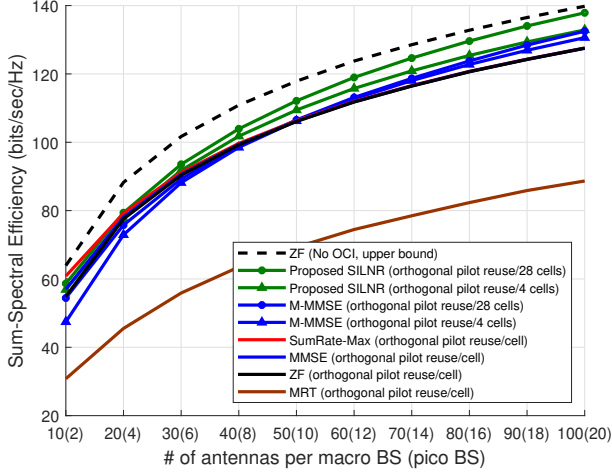


Fig. 4. The ergodic sum-spectral efficiencies for different precoding strategies when local CSIT is perfectly given.

we compare it with the sum-spectral efficiency maximization precoding and ZF when other-cell interference (OCI) is ideally eliminated. Therefore, these scheme without considering OCI serve as the upper bounds of the multicell setting, i.e., the single-cell upper bound.

Fig 4 demonstrates the ergodic sum-spectral efficiency when each BS has perfect knowledge of local CSIT, i.e., the pilot contamination effect is ignored. It is observed that the ergodic sum-spectral efficiency improves when increasing the number of antennas regardless of the precoding strategies. The proposed SILNR maximization precoding, however, provides the noticeable spectral efficiency gains compared to the existing precoding strategies, especially when the number of BS antennas is sufficiently large. These gains stem from the efficient utilization of local CSIT to mitigate both IUI and ICI to maximize the sum-spectral efficiency. In particular, the gains are magnified when having more local CSIT knowledge. This fact is because each BS can further reduce ICI as it has more local CSIT. One interesting observation is that the proposed SILNR method with channel knowledge of 10 users achieves higher sum-spectral efficiency than that attained by the M-MMSE precoding with that of 70 users. This result is also an outcome of better utilization of local CSIT. Noticeable observation is that the perfect knowledge of local CSIT is sufficient to nearly achieves the single-cell upper bound performance, provided that the number of antennas is large enough.

Fig. 5 shows the effect of imperfect CSIT caused by pilot contamination. As can be seen, the sum-spectral efficiency performances of all precoding methods are degraded compared to the perfect CSIT case. Nevertheless, the proposed SILNR maximization precoding method still outperforms the conventional precoding methods as the number of antennas per BS increases. In contrast to the perfect CSIT scenario, the SLNR precoding shows a sharp degradation of sum-spectral efficiency in the imperfect CSIT case. For instance, the SLNR precoding with imperfect channel knowledge of 70 users exhibits the poor performance than the SLNR precoding with that of 10 users. This fact implies the SLNR precoding is

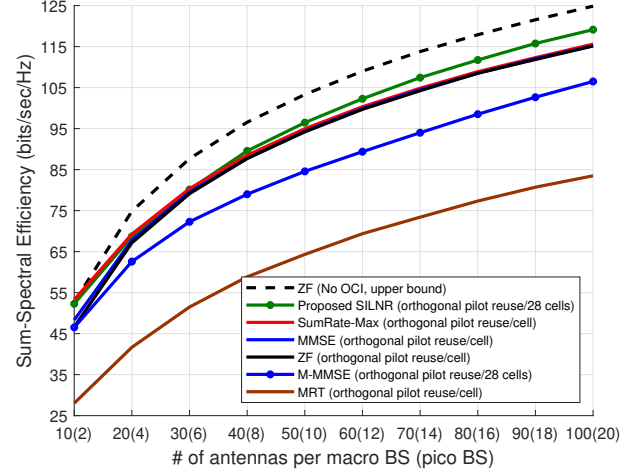


Fig. 5. The ergodic sum-spectral efficiencies for different precoding strategies with imperfect and local CSIT.

vulnerable to the pilot contamination effect. Whereas, the proposed SILNR precoding is robust to this effect by harnessing the second-order statistics of estimation error; this step yields the sum-spectral efficiency gains.

Rate distributions with perfect CSIT: Fig. 6 illustrates the distributions of ergodic spectral efficiency per user. We assume that each BS has local CSIT for 70 users, i.e., the pilot reuse over the 7 hexagonal cell areas. As can be seen, the proposed SILNR maximization achieves a better per-user rate distribution performance than the other precoding techniques, i.e., MRT, ZF, M-MMSE, and the per-cell sum-spectral efficiency maximization precoding methods. One noticeable observation is that the proposed precoding increases not only the average user rate but also the edge user rate performances. For instance, when considering the 10 percentile user rate performance, the proposed precoding method achieves about 2 bits/sec/Hz, while the other precoding techniques attain 0.8bits/sec/Hz. This implies that it improves the 10 percentile user rate performance by a factor of 2.5 times. As a result, the proposed precoding method is able to yield a much better cell-edge performance than the existing precoding solutions.

Fig. 7 illustrates the per-user rate distributions when considering pilot contamination effects is taken into account, i.e., imperfect CSIT. As can be seen, the per-user rate distribution is deteriorated by the effect of imperfect CSIT. In particular, the 10 percentile user rate performance of the proposed one becomes 1.2 bits/sec/Hz, which is 40% performance loss compared to the perfect CSIT. Nevertheless, it still outperforms the existing precoding methods considerably.

Convergence speed of the proposed SILNR maximization precoding: Fig. 8 illustrates the convergence speed of the proposed algorithm for SILNR maximization precoding. We consider the cases of $K = \{20, 40, 60\}$ and $N = 64$. We measure the mean square of the difference for the objective functions evaluated at two consecutive precoding solutions during iterations, i.e., $\mathbb{E} [\|\gamma(\mathbf{f}^{(m)}) - \gamma(\mathbf{f}^{(m-1)})\|_2^2]$ where the average is taken over both the fading channel realizations and the user locations. As depicted in Fig. 8, the number of

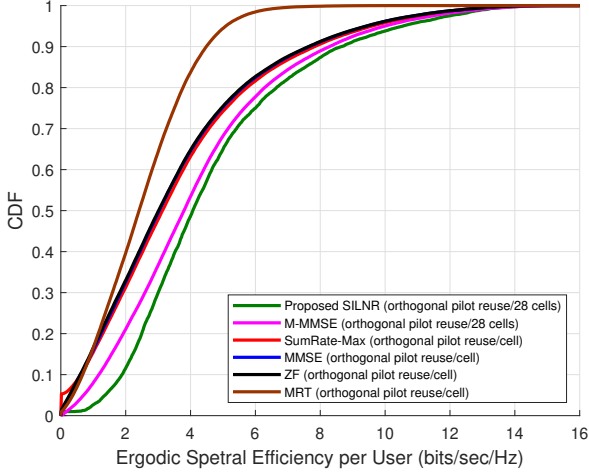


Fig. 6. The per-user rate distributions under perfect CSIT.

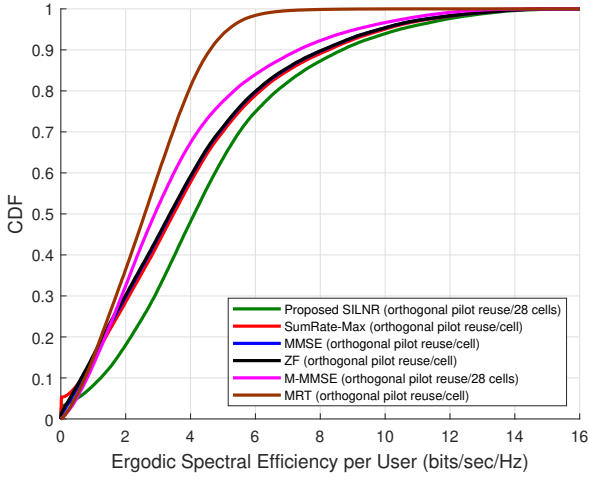


Fig. 7. The per-user rate distributions under imperfect CSIT.

required iterations to find the solution is at most five in an average sense, when we set the solution accuracy parameter to $\epsilon = 0.1$. As improving the solution accuracy level to $\epsilon = 0.01$, ten iterations are sufficient to finish the algorithm for all $K = \{20, 40, 60\}$ and $N = 64$ cases. In addition, when the algorithm starts with the ZF precoding solution as an initial point, we empirically confirm that the initially identified solution \mathbf{f}^* of Algorithm 1 has local-optimality in the most of our simulations. This fact implies that the algorithm empirically does not need the reinitialization process, which makes a fast convergence speed.

VII. CONCLUSION

In this paper, we presented a new noncooperative precoding technique using local CSIT for massive MIMO HetNets. The central idea of the proposed precoding method was to maximize the downlink sum-spectral efficiency per cell, while mitigating the other cell interference leakage using local CSIT. We introduced a new metric called SILNR that measures the ratio between the desired signal power and the superposition

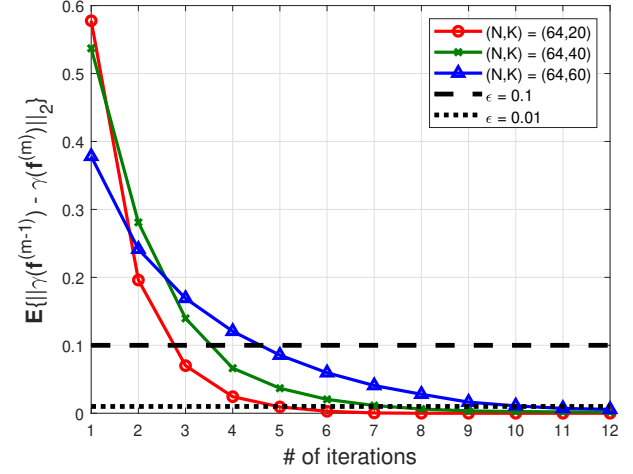


Fig. 8. Convergence speed illustration with $\epsilon = 0.1$ and $\epsilon = 0.01$.

of IUI and interference leakage powers towards the other cells. Using this metric, we formulated a maximization problem for the lower bound of the sum-spectral efficiency, which is well-known as a highly nontrivial non-convex optimization problem. We derived the first- and the second-order necessary conditions for the local optimal solution of this non-convex optimization problem. Leveraging these conditions, we presented a computationally efficient algorithm that ensures to find a local optimal solution in an iterative manner. Using both link level and system level simulations, we demonstrated that the proposed precoding method outperforms the existing noncooperative precoding strategies. One major observation was that the use of local CSIT is sufficient to mitigate both IUI and ICI in a densely deployed massive MIMO HetNets, provided that the number of antennas per BS is large enough.

APPENDIX

A. Proof for Theorem 1

Proof. To find a stationary point, we take the partial derivatives of $\gamma(\mathbf{f}_\ell)$ with respect to \mathbf{f}_ℓ and set to them zero. Let $f(\mathbf{f}_\ell) = \prod_{k=1}^{K_\ell} \mathbf{f}_\ell^H \mathbf{A}_{\ell,k} \mathbf{f}_\ell$ and $g(\mathbf{f}_\ell) = \prod_{k=1}^{K_\ell} \mathbf{f}_\ell^H \mathbf{B}_{\ell,k} \mathbf{f}_\ell$. Then,

$$\begin{aligned} \nabla_{\mathbf{f}_\ell} \gamma(\mathbf{f}_\ell) &= 0 \\ \Leftrightarrow \frac{\nabla f(\mathbf{f}_\ell) g(\mathbf{f}_\ell) - f(\mathbf{f}_\ell) \nabla g(\mathbf{f}_\ell)}{\{g(\mathbf{f}_\ell)\}^2} &= 0 \\ \Leftrightarrow \frac{g(\mathbf{f}_\ell) \sum_{i=1}^{K_\ell} \left(\prod_{k \neq i} \mathbf{f}_\ell^H \mathbf{A}_{\ell,k} \mathbf{f}_\ell \right) \mathbf{A}_{\ell,i} \mathbf{f}_\ell}{\{g(\mathbf{f}_\ell)\}^2} \\ &\quad - \frac{f(\mathbf{f}_\ell) \sum_{i=1}^{K_\ell} \left(\prod_{k \neq i} \mathbf{f}_\ell^H \mathbf{B}_{\ell,k} \mathbf{f}_\ell \right) \mathbf{B}_{\ell,i} \mathbf{f}_\ell}{\{g(\mathbf{f}_\ell)\}^2} = 0 \\ \Leftrightarrow \gamma(\mathbf{f}_\ell) \left\{ \sum_{i=1}^{K_\ell} \frac{\mathbf{A}_{\ell,i} \mathbf{f}_\ell}{\mathbf{f}_\ell^H \mathbf{A}_{\ell,i} \mathbf{f}_\ell} - \sum_{i=1}^{K_\ell} \frac{\mathbf{B}_{\ell,i} \mathbf{f}_\ell}{\mathbf{f}_\ell^H \mathbf{B}_{\ell,i} \mathbf{f}_\ell} \right\} &= 0. \end{aligned} \quad (39)$$

Rearranging the condition (39), we obtain

$$\bar{\mathbf{A}}_\ell(\mathbf{f}_\ell) \mathbf{f}_\ell = \gamma(\mathbf{f}_\ell) \bar{\mathbf{B}}_\ell(\mathbf{f}_\ell) \mathbf{f}_\ell. \quad (40)$$

This completes the proof. \square

B. Proof for Theorem 2

Proof. To prove the local-optimality claim, it is sufficient to show that the Hessian matrix at a stationary point is negative definite. To accomplish this, we first derive the Hessian matrix evaluated at an arbitrary point $\mathbf{f}_\ell \in \mathbb{C}^{N_\ell K_\ell \times 1}$, which is given by

$$\nabla_{\mathbf{f}^H}^2 \gamma(\mathbf{f}_\ell) = \nabla_{\mathbf{f}^H} \left\{ \gamma(\mathbf{f}_\ell) \left(\sum_{i=1}^{K_\ell} \frac{\mathbf{A}_i \mathbf{f}_\ell}{\mathbf{f}_\ell^H \mathbf{A}_i \mathbf{f}_\ell} - \sum_{i=1}^{K_\ell} \frac{\mathbf{B}_i \mathbf{f}_\ell}{\mathbf{f}_\ell^H \mathbf{B}_i \mathbf{f}_\ell} \right) \right\} \quad (41)$$

$$= \{ \nabla_{\mathbf{f}^H} \gamma(\mathbf{f}_\ell) \} \left(\sum_{i=1}^{K_\ell} \frac{\mathbf{A}_{\ell,i} \mathbf{f}_\ell}{\mathbf{f}_\ell^H \mathbf{A}_{\ell,i} \mathbf{f}_\ell} - \sum_{i=1}^{K_\ell} \frac{\mathbf{B}_{\ell,i} \mathbf{f}_\ell}{\mathbf{f}_\ell^H \mathbf{B}_{\ell,i} \mathbf{f}_\ell} \right)^H + \gamma(\mathbf{f}_\ell) \left\{ \nabla_{\mathbf{f}^H} \left(\sum_{i=1}^{K_\ell} \frac{\mathbf{A}_{\ell,i} \mathbf{f}_\ell}{\mathbf{f}_\ell^H \mathbf{A}_{\ell,i} \mathbf{f}_\ell} - \sum_{i=1}^{K_\ell} \frac{\mathbf{B}_{\ell,i} \mathbf{f}_\ell}{\mathbf{f}_\ell^H \mathbf{B}_{\ell,i} \mathbf{f}_\ell} \right) \right\}. \quad (42)$$

By plugging a stationary point \mathbf{f}^\star obtained from Theorem 1 into (42), it follows that

$$\nabla_{\mathbf{f}^H}^2 \gamma(\mathbf{f}_\ell^\star) = \gamma(\mathbf{f}_\ell^\star) \left\{ \nabla_{\mathbf{f}^H} \left(\sum_{i=1}^{K_\ell} \frac{\mathbf{A}_{\ell,i} \mathbf{f}_\ell^\star}{(\mathbf{f}_\ell^\star)^H \mathbf{A}_{\ell,i} \mathbf{f}_\ell^\star} - \sum_{i=1}^{K_\ell} \frac{\mathbf{B}_{\ell,i} \mathbf{f}_\ell^\star}{(\mathbf{f}_\ell^\star)^H \mathbf{B}_{\ell,i} \mathbf{f}_\ell^\star} \right) \right\} \quad (43)$$

$$= \gamma(\mathbf{f}_\ell^\star) \left\{ \sum_{i=1}^{K_\ell} \frac{\mathbf{A}_{\ell,i} \left((\mathbf{f}_\ell^\star)^H \mathbf{A}_{\ell,i} \mathbf{f}_\ell^\star \right) - 2 \mathbf{A}_{\ell,i} \mathbf{f}_\ell^\star (\mathbf{f}_\ell^\star)^H \mathbf{A}_{\ell,i}}{\left((\mathbf{f}_\ell^\star)^H \mathbf{A}_{\ell,i} \mathbf{f}_\ell^\star \right)^2} - \sum_{i=1}^{K_\ell} \frac{\mathbf{B}_{\ell,i} \left((\mathbf{f}_\ell^\star)^H \mathbf{B}_{\ell,i} \mathbf{f}_\ell^\star \right) - 2 \mathbf{B}_{\ell,i} \mathbf{f}_\ell^\star (\mathbf{f}_\ell^\star)^H \mathbf{B}_{\ell,i}}{\left((\mathbf{f}_\ell^\star)^H \mathbf{B}_{\ell,i} \mathbf{f}_\ell^\star \right)^2} \right\} \quad (44)$$

$$= \gamma(\mathbf{f}_\ell^\star) \left\{ \sum_{i=1}^{K_\ell} \frac{\mathbf{A}_{\ell,i}}{\left((\mathbf{f}_\ell^\star)^H \mathbf{A}_{\ell,i} \mathbf{f}_\ell^\star \right)} - \sum_{i=1}^{K_\ell} \frac{\mathbf{B}_{\ell,i}}{\left((\mathbf{f}_\ell^\star)^H \mathbf{B}_{\ell,i} \mathbf{f}_\ell^\star \right)} \right\} + \gamma(\mathbf{f}_\ell^\star) \left\{ \sum_{i=1}^{K_\ell} \frac{-2 \mathbf{A}_{\ell,i} \mathbf{f}_\ell^\star (\mathbf{f}_\ell^\star)^H \mathbf{A}_{\ell,i}}{\left((\mathbf{f}_\ell^\star)^H \mathbf{A}_{\ell,i} \mathbf{f}_\ell^\star \right)^2} + \sum_{i=1}^{K_\ell} \frac{2 \mathbf{B}_{\ell,i} \mathbf{f}_\ell^\star (\mathbf{f}_\ell^\star)^H \mathbf{B}_{\ell,i}}{\left((\mathbf{f}_\ell^\star)^H \mathbf{B}_{\ell,i} \mathbf{f}_\ell^\star \right)^2} \right\}. \quad (45)$$

In (45), the first terms $\gamma(\mathbf{f}_\ell^\star) \left\{ \sum_{i=1}^{K_\ell} \frac{\mathbf{A}_{\ell,i}}{(\mathbf{f}_\ell^\star)^H \mathbf{A}_{\ell,i} \mathbf{f}_\ell^\star} - \sum_{i=1}^{K_\ell} \frac{\mathbf{B}_{\ell,i}}{(\mathbf{f}_\ell^\star)^H \mathbf{B}_{\ell,i} \mathbf{f}_\ell^\star} \right\}$ become zero from the result of Theorem 1. As a result, the Hessian matrix simplifies to

$$\nabla_{\mathbf{f}^H}^2 \gamma(\mathbf{f}_\ell^\star) = 2\gamma(\mathbf{f}_\ell^\star) \left\{ \sum_{i=1}^{K_\ell} \frac{\mathbf{B}_{\ell,i} \mathbf{f}_\ell^\star (\mathbf{f}_\ell^\star)^H \mathbf{B}_{\ell,i}}{\left((\mathbf{f}_\ell^\star)^H \mathbf{B}_{\ell,i} \mathbf{f}_\ell^\star \right)^2} - \sum_{i=1}^{K_\ell} \frac{\mathbf{A}_{\ell,i} \mathbf{f}_\ell^\star (\mathbf{f}_\ell^\star)^H \mathbf{A}_{\ell,i}}{\left((\mathbf{f}_\ell^\star)^H \mathbf{A}_{\ell,i} \mathbf{f}_\ell^\star \right)^2} \right\}. \quad (46)$$

In (46), the first term $\gamma(\mathbf{f}^\star)$ is a positive scalar value and all the remaining terms are the summation of positive-definite matrices because $\mathbf{A}_{\ell,i}$ and $\mathbf{B}_{\ell,i}$ are the Hermitian matrices. It means that if the minimum eigenvalue of $\sum_{i=1}^{K_\ell} \frac{\mathbf{A}_{\ell,i} \mathbf{f}_\ell^\star (\mathbf{f}_\ell^\star)^H \mathbf{A}_{\ell,i}}{\left((\mathbf{f}_\ell^\star)^H \mathbf{A}_{\ell,i} \mathbf{f}_\ell^\star \right)^2}$ is bigger than the maximum eigenvalue of the $\sum_{i=1}^{K_\ell} \frac{\mathbf{B}_{\ell,i} \mathbf{f}_\ell^\star (\mathbf{f}_\ell^\star)^H \mathbf{B}_{\ell,i}}{\left((\mathbf{f}_\ell^\star)^H \mathbf{B}_{\ell,i} \mathbf{f}_\ell^\star \right)^2}$, then

the Hessian matrix $\nabla_{\mathbf{f}^H}^2 \gamma(\mathbf{f}_\ell^\star)$ is sufficient to be a negative-definite matrix. This completes the proof. \square

REFERENCES

- [1] A. Ghosh, N. Mangalvedhe, R. Ratasuk, B. Mondal, M. Cudak, E. Vitsosky, T. A. Thomas, J. G. Andrews, P. Xia, H. S. Jo, H. S. Dhillon, and T. D. Novlan, "Heterogeneous cellular networks: From theory to practice," *IEEE Commun. Mag.*, vol. 50, no. 6, pp. 54–64, 2012.
- [2] H. S. Dhillon, M. Kountouris, and J. G. Andrews, "Downlink MIMO HetNets: Modeling, ordering results and performance analysis," *IEEE Trans. Wireless Commun.*, vol. 12, no. 10, pp. 5208–5222, 2013.
- [3] J. G. Andrews, S. Singh, Q. Ye, X. Lin, and H. S. Dhillon, "An overview of load balancing in HetNets: Old myths and open problems," *IEEE Wireless Commun. Mag.*, vol. 21, no. 2, pp. 18–25, 2014.
- [4] K. Hosseini, J. Hoydis, S. Ten Brink, and M. Debbah, "Massive MIMO and small cells: How to densify heterogeneous networks," in *Proc. IEEE Int. Conf. Commun. (ICC)*, June 2013, pp. 5442–5447.
- [5] N. Chen, B. Rong, X. Zhang, and M. Kadoch, "Scalable and flexible massive MIMO precoding for 5G H-CRAN," *IEEE Wireless Commun. Mag.*, vol. 24, no. 1, pp. 46–52, 2017.
- [6] A. Adhikary, H. S. Dhillon, and G. Caire, "Spatial blanking and inter-tier coordination in massive MIMO heterogeneous cellular networks," in *Proc. IEEE Globecom Workshops (GC Wkshps)*, Dec 2014, pp. 1229–1234.
- [7] D. Lopez-Perez, I. Guvenc, G. de la Roche, M. Kountouris, T. Quek, and J. Zhang, "Enhanced intercell interference coordination challenges in heterogeneous networks," *IEEE Wireless Commun. Mag.*, vol. 3, no. 18, pp. 22–30, 2011.
- [8] A. K. Gupta, H. S. Dhillon, S. Vishwanath, and J. G. Andrews, "Downlink multi-antenna heterogeneous cellular network with load balancing," *IEEE Trans. Commun.*, vol. 62, no. 11, pp. 4052–4067, 2014.
- [9] A. Adhikary, J. Nam, J.-Y. Ahn, and G. Caire, "Joint spatial division and multiplexing the large-scale array regime," *IEEE Trans. Inf. Theory*, vol. 59, no. 10, pp. 6441–6463, 2013.
- [10] E. G. Larsson, O. Edfors, F. Tufvesson, and T. L. Marzetta, "Massive MIMO for next generation wireless systems," *IEEE Commun. Mag.*, vol. 52, no. 2, pp. 186–195, 2014.
- [11] F. Rusek, D. Persson, B. Lau, E. Larsson, T. Marzetta, O. Edfors, and F. Tufvesson, "Scaling up MIMO: Opportunities and challenges with very large arrays," *IEEE Signal Process. Mag.*, vol. 30, pp. 40–60, 2013.
- [12] T. L. Marzetta, "Noncooperative cellular wireless with unlimited numbers of base station antennas," *IEEE Trans. Wireless Commun.*, vol. 9, no. 11, pp. 3590–3600, 2010.
- [13] J. Hoydis, S. ten Brink, and M. Debbah, "Massive MIMO in the UL/DL of cellular networks: How many antennas do we need?" *IEEE J. Sel. Areas Commun.*, vol. 31, no. 2, 2013.
- [14] T. K. Lo, "Maximum ratio transmission," in *Proc. IEEE Int. Conf. Commun. (ICC)*, vol. 2, June 1999, pp. 1310–1314.
- [15] E. Björnson, L. Sanguinetti, J. Hoydis, and M. Debbah, "Designing multi-user MIMO for energy efficiency: When is massive MIMO the answer?" in *Proc. IEEE Wireless Commun. Netw. Conf. (WCNC)*, April 2014, pp. 242–247.
- [16] Y.-G. Lim, C.-B. Chae, and G. Caire, "Performance analysis of massive MIMO for cell-boundary users," *IEEE Trans. Wireless Commun.*, vol. 14, no. 12, pp. 6827–6842, 2015.
- [17] Q. H. Spencer, A. L. Swindlehurst, and M. Haardt, "Zero-forcing methods for downlink spatial multiplexing in multiuser MIMO channels," *IEEE Trans. Signal Process.*, vol. 52, no. 2, pp. 461–471, 2004.
- [18] T. Yoo and A. Goldsmith, "On the optimality of multi-antenna broadcast scheduling using zero-forcing beamforming," *IEEE J. Sel. Areas Commun.*, vol. 24, no. 3, pp. 528–541, 2006.
- [19] M. Costa, "Writing on dirty paper (corresp.)," *IEEE Trans. Inf. Theory*, vol. 29, no. 3, pp. 439–441, 1983.
- [20] T. E. Bogale and L. B. Le, "Massive MIMO and mmWave for 5G wireless HetNet: Potential benefits and challenges," *IEEE Veh. Technol. Mag.*, vol. 11, no. 1, pp. 64–75, 2016.
- [21] M. Sadek, A. Tarighat, and A. H. Sayed, "A leakage-based precoding scheme for downlink multi-user MIMO channels," *IEEE Trans. Wireless Commun.*, vol. 6, no. 5, pp. 1711–1721, 2007.
- [22] J. Jose, A. Ashikhmin, T. L. Marzetta, and S. Vishwanath, "Pilot contamination and precoding in multi-cell TDD systems," *IEEE Trans. Wireless Commun.*, vol. 10, no. 8, pp. 2640–2651, 2011.
- [23] P. Patcharamaneepakorn, S. Armour, and A. Doufexi, "On the equivalence between SLNR and MMSE precoding schemes with single-antenna receivers," *IEEE Commun. Lett.*, vol. 16, no. 7, pp. 1034–1037, 2012.

- [24] E. Björnson, J. Hoydis, and L. Sanguinetti, "Massive MIMO has unlimited capacity," *IEEE Trans. Wireless Commun.*, vol. 17, no. 1, pp. 574–590, 2017.
- [25] E. Björnson and L. Sanguinetti, "A new look at cell-free massive MIMO: Making it practical with dynamic cooperation," in *Proc. IEEE Annu. Int. Symp. Pers., Indoor and Mobile Radio Commun. (PIMRC)*, Sep. 2019, pp. 1–6.
- [26] S. S. Christensen, R. Agarwal, E. De Carvalho, and J. M. Cioffi, "Weighted sum-rate maximization using weighted MMSE for MIMO-BC beamforming design," *IEEE Trans. Wireless Commun.*, vol. 7, no. 12, pp. 4792–4799, 2008.
- [27] J. Choi, N. Lee, S.-N. Hong, and G. Caire, "Joint user scheduling, power allocation, and precoding design for massive MIMO systems: A principal component analysis approach," in *Proc. IEEE Int. Symp. Inf. Theory (ISIT)*, June 2018, pp. 396–400.
- [28] —, "Joint user selection, power allocation, and precoding design with imperfect CSIT for multi-cell MU-MIMO downlink systems," *IEEE Trans. Wireless Commun. (Early Access)*, 2019.
- [29] H. Yin, D. Gesbert, M. Filippou, and Y. Liu, "A coordinated approach to channel estimation in large-scale multiple-antenna systems," *IEEE J. Sel. Areas Commun.*, vol. 31, no. 2, pp. 264–273, 2013.
- [30] J. Hoydis, S. Ten Brink, and M. Debbah, "Massive MIMO: How many antennas do we need?" in *Proc. 49th Annu. Allerton Conf. Commun., Control, and Comput. (Allerton)*, Sep. 2011, pp. 545–550.
- [31] T. Yoo and A. Goldsmith, "Capacity and power allocation for fading MIMO channels with channel estimation error," *IEEE Trans. Inf. Theory*, vol. 52, no. 5, pp. 2203–2214, 2006.
- [32] M. Medard, "The effect upon channel capacity in wireless communications of perfect and imperfect knowledge of the channel," *IEEE Trans. Inf. Theory*, vol. 46, no. 3, pp. 933–946, 2000.
- [33] A. Lapidoth and S. Shamai, "Fading channels: How perfect need perfect side information be?" *IEEE Trans. Inf. Theory*, vol. 48, no. 5, pp. 1118–1134, 2002.
- [34] M. Ding and S. D. Blostein, "Maximum mutual information design for MIMO systems with imperfect channel knowledge," *IEEE Trans. Inf. Theory*, vol. 56, no. 10, pp. 4793–4801, 2010.
- [35] C. Lim, T. Yoo, B. Clerckx, B. Lee, and B. Shim, "Recent trend of multiuser MIMO in LTE-advanced," *IEEE Communications Magazine*, vol. 51, no. 3, pp. 127–135, 2013.
- [36] R. Zhang, K. Giridhar, and L. Hanzo, "Distributed downlink multi-cell processing requiring reduced-rate back-haul data exchange," in *Proc. IEEE Wireless Commun. Netw. Conf. (WCNC)*, March 2011, pp. 1277–1281.
- [37] R. Zhang and L. Hanzo, "Cooperative downlink multicell preprocessing relying on reduced-rate back-haul data exchange," *IEEE Trans. Veh. Technol.*, vol. 60, no. 2, pp. 539–545, 2010.
- [38] F. Fernandes, A. Ashikhmin, and T. L. Marzetta, "Inter-cell interference in noncooperative TDD large scale antenna systems," *IEEE J. Sel. Areas Commun.*, vol. 31, no. 2, pp. 192–201, 2013.
- [39] W. Shin, N. Lee, J.-B. Lim, C. Shin, and K. Jang, "On the design of interference alignment scheme for two-cell MIMO interfering broadcast channels," *IEEE Trans. Wireless Commun.*, vol. 10, no. 2, pp. 437–442, 2010.